Arabian Journal of Chemistry (2021) **14**, 103059

King Saud University

Arabian Journal of Chemistry

www.ksu.edu.sa
www.sciencedirect.com

ORIGINAL ARTICLE

Heat absorption properties of $CuO/TiO_2/SiO_2$ trihybrid nanofluids and its potential future direction towards solar thermal applications

Nur Alya Syamimie Muzaidi [a], Mohd Amiruddin Fikri [a], Khairul Nizar Syazwan Wan Salihin Wong [b,d], Azfi Zaidi Mohammad Sofi [a], Rizalman Mamat [c], Norfatihah Mohd Adenam [a], Muhamad Yuzaini Azrai Mat Yunin [a], Hasyiya Karimah Adli [b,d,*]

[a] *Faculty of Bioengineering and Technology, Universiti Malaysia Kelantan, 17600 Jeli, Kelantan, Malaysia*
[b] *Institute for Artificial Intelligence and Big Data, Universiti Malaysia Kelantan, City Campus, Pengkalan Chepa, 16100 Kota Bharu, Kelantan, Malaysia*
[c] *Department of Mechanical Engineering, College of Engineering, Universiti Malaysia Pahang, Lebuhraya Tun Razak, 26300 Gambang, Kuantan, Pahang, Malaysia*
[d] *Department of Data Science, Universiti Malaysia Kelantan, City Campus, Pengkalan Chepa, 16100 Kota Bharu, Kelantan, Malaysia*

Received 21 September 2020; accepted 1 February 2021
Available online 11 February 2021

KEYWORDS

Trihybrid;
Nanofluids;
Heat absorption;
Temperature output

Abstract In this study, we investigated the physical properties of $CuO/TiO_2/SiO_2$ trihybrid nanofluids. The physical properties that were investigated included density, crystallite size, and surface morphology. The trihybrid nanofluid density was observed to increase at higher volume concentration, with **t1** exhibiting the highest density (2.26 gml^{-1}). X-Ray Diffraction (XRD) spectra showed the main diffraction peaks of individual nanoparticles (CuO, TiO_2 and SiO_2), highlighting the successful formation of trihybrid nanoparticles. The nanofluid's calculated crystallite size showed the formation of smaller trihybrid nanofluid crystallites (5.2 nm) compared to the original nanoparticles. The crystallite size is in good agreement with the SEM surface morphology, which shows the appearance of small particles. The trihybrid solution (**t1**) had the best thermal properties, based on temperature output, at around 55 °C, as the highest volume concentration of nanofluids was used. The heat absorption of **t1** also demonstrated increased temperature output at higher solar

* Corresponding author at: Institute for Artificial Intelligence and Big Data, Universiti Malaysia Kelantan, City Campus, Pengkalan Chepa, 16100 Kota Bharu, Kelantan, Malaysia.
E-mail address: hasyiya@umk.edu.my (H.K. Adli).
Peer review under responsibility of King Saud University.

Production and hosting by Elsevier

https://doi.org/10.1016/j.arabjc.2021.103059

radiations with a maximum temperature output at 73 °C under 700 W/m^2. This study is the first to report on the thermal properties CuO/TiO_2/SiO_2 trihybrid nanofluids for future solar thermal application.

1. Introduction

Cumulatively, fossil fuels accounted for 84% of the world's primary energy source in 2019. Fossil fuels also dominated about 40% of global electricity generation in the same year (BP Statistical Review of World Energy, 2020). Global electrical energy consumption is typically high, and the demand is growing rapidly at an alarming rate. In an effort to reduce the dependency on fossil fuels, many countries have turned to renewable energy such as solar energy (Grätzel, 2009). Generating electricity with solar power instead of fossil fuels can dramatically reduce greenhouse gas emissions, particularly carbon dioxide (CO_2). Greenhouse gases emitted by fossil fuels have led to increased global temperature and climate change, subsequently contributing to serious environmental and public health issues (Haines et al., 2006).

Solar water heating is currently the most common application of solar energy systems, especially in urban areas. This system is environmentally friendly and harnesses the generated electricity to heat water (Shukla et al., 2013). Basically, this system involves natural solar thermal technology based on simple working principles that require only sunlight to heat the water. The system works by bringing the thermal fluid into contact with a dark surface exposed to sunlight, which then increases the temperature of the fluid (Al-Badi and Albadi, 2012). In a direct system, the fluid may cause the water to heat up directly, or in an indirect system, a heat transfer fluid (e.g., glycol or a water mixture) could be used to pass through some form of heat exchanger (Jamar et al., 2016).

Meanwhile, nanofluids are world-class heat transfer working fluids that have been developed by adding solid nanoparticles to the base fluids (Alawi et al., 2018; Sarafraz et al., 2019). Homogenized mixtures of low-volume-fraction nanoparticles and conventional fluids such as ethylene glycol, glycerine, oil, and water can remarkably increase overall thermal performance (Das et al., 2007; Sarafraz et al., 2016). Due to its potential use in numerous engineering applications, nanofluids are now the focus of an expanding body of research. Additionally, nanofluids are most commonly used in heating and cooling processes prevalently seen in solar cells, solar stills, and other thermal energy storage methods (Khanafer and Vafai, 2018; Sarafraz et al., 2018) and thermal conductivity (Ghalambaz et al., 2020a, 2020b).

Oxide nanofluids such as aluminum oxide (Al_2O_3), titanium oxide (TiO_2), silicon dioxide (SiO_2), and copper oxide (CuO) are mostly used in heat transfer applications either as single or hybrid nanofluids, due to their capability to increase heat transfer in the heat transfer system by up to 60% (Azmi et al., 2019). The investigation into various hybrid nanofluid applications have greatly increased (Fikri et al., 2020b). Hybrid or composite nanofluids are an extension of the body of research on single nanofluids. These hybrids can be made via two or more different nanoparticles: either in the form of a mixture or a composite that disperses in liquid (Minea, 2017). Previous works have reported on the superiority of the thermal and rheological properties of hybrid and composite nanofluids over single nanoparticles. Table 1 presents the summary of respective nanofluids for thermal properties characterization.

Thus, it can be summarized that oxides have great promise in solar thermal applications and the hybrid nanofluids have superior thermophysical properties over single nanofluids. Based on the above findings, this study aims to develop a novel, trihybrid nanofluids made up of CuO, TiO_2, and SiO_2 and to investigate the physical properties of these materials such as density, crystallite size, and surface morphology, as well as temperature output performance. This is the first study to report on the CuO/TiO_2/SiO_2 trihybrid nanofluid. Thus, this study is the first to report on the thermal properties CuO/TiO_2/SiO_2 trihybrid nanofluids for future solar thermal application.

2. Experimental method

2.1. Materials preparation

Copper (II) oxide powder (Bendosen) (99.9%, ≤ 160 μm), titanium dioxide (TiO_2) powder (R&M chemicals) (≥99.5%, 1 to 150 nm) and silicon dioxide (SiO_2) powder (HmbG Chemical) (99.9%, 0–2000 μm) were used without further purification. Initially, each nanofluid from the copper oxide (CuO), titanium dioxide (TiO_2), and silicon dioxide (SiO_2) nanoparticles was prepared in 2.5 M that were dissolved in ethylene glycol. Then, the mixture was stirred continuously for 3 days and sonicated for 2 h until a homogenized solution was obtained. Each nanofluid was mixed at a 1:3 vol ratio to finally form 100 mL of the (CuO/TiO_2/SiO_2) trihybrid nanofluids. Different concentrations of the trihybrid nanofluids were prepared in water and ethylene glycol mixture (60:40) which are 0.17, 0.08 and 0.04 M, denoted as **t1**, **t2,** and **t3** respectively. The overall process is summarized in Fig. A1.

2.2. Physical characterization

The investigation into the physical properties of the prepared (CuO/TiO_2/SiO_2) trihybrid nanofluids (**t1**, **t2,** and **t3**) was observed via visualization effect (Chakraborty and Panigrahi, 2020). Sedimentation is the most commonly used technique for stability evaluation which based on the formation of sediment at the bottom of the liquid column due to gravity. The longer time taken by the nanofluid for the formation of precipitate is an indication of superior stability of nanofluid. Several researchers have used the sedimentation technique to evaluate nanofluid stability (Chakraborty et al., 2018a, 2018b). The

Table 1 Summary of experimental results of thermal properties measurement of various nanofluids.

Particle	Type	Base fluid	Enhancement	References
Al_2O_3	Single	Ethylene glycol	The thermal conductivity decreased when the EG content in the mixture increased, but increased when the volume concentration of the Al_2O_3 nanofluids increased	Hamid et al. (2018)
	Single	Water and ethylene glycol	The average thermal conductivity enhancement from 2.6 to 12.8% as the percentage of ethylene glycol increases	Chiam et al. (2017)
	Single	Ethylene glycol and water	At fixed EG content, the thermal conductivity of nanofluids increased with increasing of temperature	Guo et al. (2018)
SiO_2	Single	Ethylene glycol	Viscosity linearly increased with the increased of nanoparticles concentration with maximum enhancement with 1.3905 times	Żyła and Fal (2017)
TiO_2	Single	Water, ethylene glycol, paraffin oil	The thermal conductivity increases 22% with the addition of nanoparticles	Sonawane et al. (2015)
	Single	Ethylene glycol	Thermal conductivity and viscosity of nanofluids increased with the addition of nanoparticles to base fluids	Khedkar et al. (2016)
CuO	Single	Water, ethylene glycol, engine oil	Thermal conductivity increases 40%, 27% and 19%, for CuO in water, EG and engine oil, respectively	Agarwal et al. (2016)
	Single	Water	18% increase in thermal conductivity	Nemale and Waghuley (2016)
Al_2O_3, TiO_2, SiO_2 and CuO	Single	Ethylene glycol, water	The thermal conductivity of oxide nanofluids was enhanced up to 40% better than the base fluids (water)	Azmi et al. (2019)
Al_2O_3 and SiO_2	Hybrid	Water	An increase of thermal conductivity with volume fraction and temperature increase	Moldoveanu et al. (2018)
ZnO and TiO_2	Hybrid	Ethylene glycol (0.1–3.5 vol%)	Maximum enhancement (32%) at ϕ = 3.5% and 50 °C	Toghraie et al. (2016)
SiO_2 and TiO_2	Hybrid	Water and ethylene glycol (60:40)	Maximum enhancement of 22.8% obtained at 3.0% volume concentration and 80 °C temperature.	Nabil et al. (2018)
	Hybrid	Water and ethylene glycol (60:40)	The nanofluid viscosity increased with increased volume concentration and decreased with increased temperature	Hamid et al. (2019) and Guo et al. (2018)
	Hybrid	Ethylene glycol and water (40:60)	The maximum enhancement 22.1% at concentration 3.0% and temperature 70 °C	Hamid et al. (2017)
TiO_2 and Al_2O_3	Hybrid	Water	The highest thermal conductivity value of 1.134 W/m K is observed for hybrid nanofluid with mixing ratio of 50:50 at 70 °C, with an average thermal conductivity augmentation of 71% comparative to deionized (DI) water	Wanatasanapan et al. (2020)
	Hybrid	Ethylene glycol and water (40:60)	The thermal conductivity is improved by 40.86% at 0.1% volume concentration and 80 °C	Urmi et al. (2020)
Al_2O_3, TiO_2 and SiO_2	Trihybrid	Water and Ethylene glycol (60:40)	Reported trihybrid nanofluids remains stable with a concentration ratio of 80%.	Ramadhan et al. (2019)
	Trihybrid	Water and Ethylene glycol (60:40)	The maximum enhancement of the heat transfer coefficient for coolant side is observed at 39.7% at 0.3% volume concentration	Ramadhan et al. (2020)
SiO_2, Al_2O_3 and ZrO_2	Trihybrid	Deionised water and Ethylene glycol (60:40)	Nanofluid viscosity decreases with increasing liquid temperature and increases with increasing of nanoparticles volume concentration	Safiei et al. (2020)

density of the base fluids and the prepared trihybrid nanofluids was checked using a density meter (Radwag Balances and Scales model), and several physical characterizations were conducted via Ultraviolet–visible Spectrophotometer (UV–vis), X-Ray Diffraction (XRD), and Scanning Electron Microscopy (SEM). MeaUV–Vis analysis was carried out using a Spectroquant Pharo 300 UV–vis Spectrometer. This analysis was run 10 days in a row with a wavelength set at 400 nm to determine the absorption and the stability of the trihybrid nanofluid. The crystallite size and the crystalline structure of CuO, TiO_2, and SiO_2, as well as the **t1**, **t2,** and **t3** trihybrid were determined via X-ray diffraction (XRD D2 Phaser, Bruker). The surface morphology was observed using a JEOL JSM IT 100 Scanning Electron Microscope (SEM) at 300× magnification.

2.3. Heat absorption performance

t1, **t2** and **t3** trihybrid nanofluids were exposed to 300 W/m^2 artificial solar radiation to investigate the heat absorption performance of each nanofluid, after which **t1** was chosen for further analysis on different solar radiation intensities (300 W/m^2, 500 W/m^2, and 700 W/m^2). A dimmer switch was installed in the circuit to regulate the solar radiation. The experiment started with a charging process of 16 min and then a discharging process for another 16 min using a thermocouple. The temperature data was recorded every 2 min in a controlled environment. The temperature was displayed by thermocouple and the information was manually recorded. The experimental setup is shown in Fig. A2, with detailed descriptions given in Table A1.

3. Results and discussion

3.1. Physical properties

The formulation of the trihybrid nanofluids is based on the two-step method outlined by Ramadhan et al. (2019), with the difference of metal oxides and solution concentrations used. The copper oxide (CuO), titanium dioxide (TiO_2), and silicon dioxide (SiO_2) solutions in ethylene glycol were prepared individually before mixing to finally form the ($CuO/TiO_2/SiO_2$) trihybrid solution. Fig. A1 shows the image of oxide solution and trihybrids solutions.

Ethylene glycol also acts as an antifreeze when mixed with water to form a solution with a relatively good heat transfer (Peyghambarzadeh et al., 2011). Ethylene glycol (EG) has been reported to minimize the damage and increase the shelf-life of water heating systems (Sundar et al., 2014). According to the literature, mixed base fluids have better heat transfer properties with high thermal conductivity and low viscosity. The use of base-water has limited operated temperature range, high vapour pressure and high corrosivity. Besides, ethylene glycol has higher performance in the convective heat transfer compared to water. Thus, a water-ethylene glycol mixture at a 60:40 ratio was used as the base fluid for this study.

The density of the base fluids used in this study was initially checked to compare the density of distilled water with the distilled water-ethylene glycol mixture, as shown in Table A2. Next, the density of the prepared **t1**, **t2,** and **t3** trihybrid was measured. It was found that the density increased with increasing nanoparticle concentration. According to the rule of mixtures, the density of good heat transfer fluids increases linearly with volume fraction since the addition of a small fraction of solid nanoparticles to the base liquid will enhance the density of the mixture (Chandrasekar et al., 2012; Tahat and Benim, 2017).

Fig. A3 shows the images of **t1**, **t2** and **t3** trihybrid nanofluids with concentrations of 0.17, 0.08 and 0.04 M, respectively, at after preparation (day 1) and at day 10. At room temperature, no sedimentation of particles was observed after the solution was prepared but sedimentation started to form on day 10. The sedimentation was occurred due to the effect of gravity on the particles (Sahid et al., 2017). The suspension of these solid particles in the base fluids reported can enhance the energy transmission in the fluids resulting an increase thermal conductivity properties and heat transfer performance (Ganji et al., 2018; Okonkwo et al., 2019).

3.2. Physical characterization

Fig. A4 displays the X-Ray Diffraction (XRD) patterns of CuO, TiO_2, SiO_2, and the ($CuO/TiO_2/SiO_2$) trihybrid collected within a Bragg's angle (2θ) between 10° and 90°. The diffraction pattern in Fig. A4(a) is identical to the single-phase monoclinic CuO observed at $2\theta \approx 32°$ and 35°, indicating the good crystallinity of the copper oxide nanoparticles. All diffraction peaks of CuO at (32, 35, 38, 48, 53, 58, 61 and 67) ° are in good agreement with the JCPDS card NO. 48-1548 (Siddiqui et al., 2018). Next, the peak of the SiO_2 nanoparticles was observed at $2\theta \approx 24°$ reported in amorphous phase (Yuvakkumar et al., 2014; Nayak et al., 2019), while the sharp peak of TiO_2 nanoparticles at $2\theta \approx 25°$, 38°, and 48° confirm the presence of the anatase phase in concordance with the JCPDS card no.: 21-1272 and 211,276 database (Li et al., 2014; Almashhori et al., 2020; Antić et al., 2012). Meanwhile, the XRD spectrum of the ($CuO/TiO_2/SiO_2$) trihybrid (Fig. A4d) shows the appearance of the main diffraction peaks from the individual nanoparticles (CuO, TiO_2 and SiO_2), highlighting the formation of the trihybrid nanoparticles. The diffraction peaks were observed at $2\theta \approx 25°$, 35°, 38°, 48°, and 54°.

The crystallite size of the nanoparticles was identified from XRD patterns according to the peak position (Zak et al., 2012). The crystallite size of the nanofluids was evaluated by measuring the FWHM of the strongest peak (Mohammadi et al., 2017). The average crystallite size was computed using the Debye–Scherrer formula below (Deraz and Abd-Elkader, 2014):

$$D = k\lambda/\beta\cos\theta$$

where D is the crystallite size (nm), k is a constant equal to 0.9, λ is the wavelength of X-ray radiation (0.15406 nm), β is the full-width at half maximum (FWHM) of the peak (in radians), and θ is peak position (in radians).

Based on the FWHM values, the calculated average crystallite size of CuO, SiO_2, TiO_2, and the trihybrid was 26.4 nm, 0.6 nm, 14.4 nm, and 5.2 nm, respectively. From the results obtained (Table A3), it can be concluded that the trihybrid particles had a smaller crystallite size (5.2 nm) compared to their original nanoparticles.

From Fig. A5(a), the surface morphology of the CuO nanoparticles is spherical and nearly uniform in size, with a similar shape to that reported previously (Ranjbar-Karimi et al., 2010). This spherical nanoparticle form is favorable for the heat transfer of absorbed solar energy within the nanofluid and can increase solar absorption capacity (Subramaniyan et al., 2018). Meanwhile, Fig. A5 (b) and (c) show the images of the SiO_2 and TiO_2 nanoparticles that are also similar in shape to that reported by Ramadhan et al. (2019). The surface morphology of $CuO/TiO_2/SiO_2$ in Fig. A5(d) appear similar in shape to that of the (CuO, TiO_2 and SiO_2) original nanoparticles, proving the formation of the trihybrid nanoparticles although the size of CuO changed after the trihybrid formation. The spherical, nearly uniform size, and rock-like shape, as well as the smaller crystallite particles, prove that the nanoparticles are loose agglomerates (Akilu et al., 2017).

The absorption spectra of the trihybrid nanofluid in different volume concentrations were determined using a UV–Vis spectrophotometer at 400 nm for up to 10 days at room temperature to optimize the stability of the nanohybrid solutions. The absorbance of the nanofluids was found to linearly increase with an increase in volume concentration. This trend is in agreement with the Beer-Lambert Law (Sharif et al., 2019). The UV–vis absorption of the 0.05% (**t3**), 0.1% (**t2**), and 0.2% (**t1**) concentrations are shown in Fig. A6. From the UV–vis spectrum, **t1** clearly recorded the highest UV–vis absorption, as **t1** has the highest concentration of the sample series. The mixing solution was confirmed due to the comparison of spectra made based on the literature (Saidina et al., 2020; Kumar et al., 2020; Adam et al., 2020). Furthermore, the absorbance of the trihybrid nanofluids in different concentrations was monitored after 24 h up until day 10 (240 h). It was found that the absorbance of the $CuO/TiO_2/SiO_2$ trihybrid (**t1**, **t2,** and **t3**) decreased over hours (Fig. A7). On day

5, **t2** was the most stable trihybrid with only a 10.5% decrease, compared to **t3** (60%) and **t1** (27.6%). However, nearing 240 h, **t1** showed the highest absorption of the series, with only a 62.1% drop in the initial absorbance reading.

3.3. Heat absorption performance analysis

Fig. A8 shows the comparison of solar absorption and the cooling curve of the base fluids, the distilled water (dw), and the mixture of distilled water and ethylene glycol (w:eg), carried out under 15 min charging and 15 min discharging. The results clearly show w:eg having better base fluid properties so it will store heat better than dw.

In a similar method, the heat absorption performance of the (**t1**, **t2**, and **t3**) trihybrid nanofluids in water-ethylene glycol as the base fluid was investigated under 300 W/m^2 solar radiation. From the analysis, the temperature gradually increased with time during the charging process and started to decrease during the discharge process (Fig. A9a). Hence, **t1** recorded the highest performance due to its highest concentration of nanofluids and thus the best thermal absorber of the series. Under different solar radiation (Fig. A9b), **t1** exhibited increasing heat absorption at higher solar radiation (500 W/m^2) and 700 W/m^2) with a maximum temperature achieved at 73 °C. In summary, the obtained results exhibited improved performance in thermophysical properties, compared to the TiO_2-SiO_2 hybrid nanofluids, which recorded a maximum temperature of 37 °C under 300 W/m^2 solar radiation (Fikri et al. 2020a, 2020b).

4. Conclusion

A trihybrid nanofluid was successfully prepared from CuO, TiO_2, and SiO_2 and analyzed using XRD, SEM, UV–vis, and thermocouple. **t1** recorded the highest density of 2.26 gml^{-1}. The XRD spectra showed the existence of the main diffraction peaks of the individual nanoparticles (CuO, TiO_2, and SiO_2), proving the formation of the $CuO/TiO_2/SiO_2$ trihybrid. The calculated crystallite size and SEM images demonstrated the smaller size of the trihybrid nanoparticles (5.2 nm) compared to the original size of their oxides. The as-prepared trihybrid nanofluid solution (**t1**) performed stably for 240 h, with only a 62.1% drop in the initial absorbance reading. From the heat absorption performance, **t1** recorded the best performance, achieving maximum temperature at 73 °C under 700 W/m^2.

Declaration of Competing Interest

The authors declare that they have no known competing financial interests or personal relationships that could have appeared to influence the work reported in this paper.

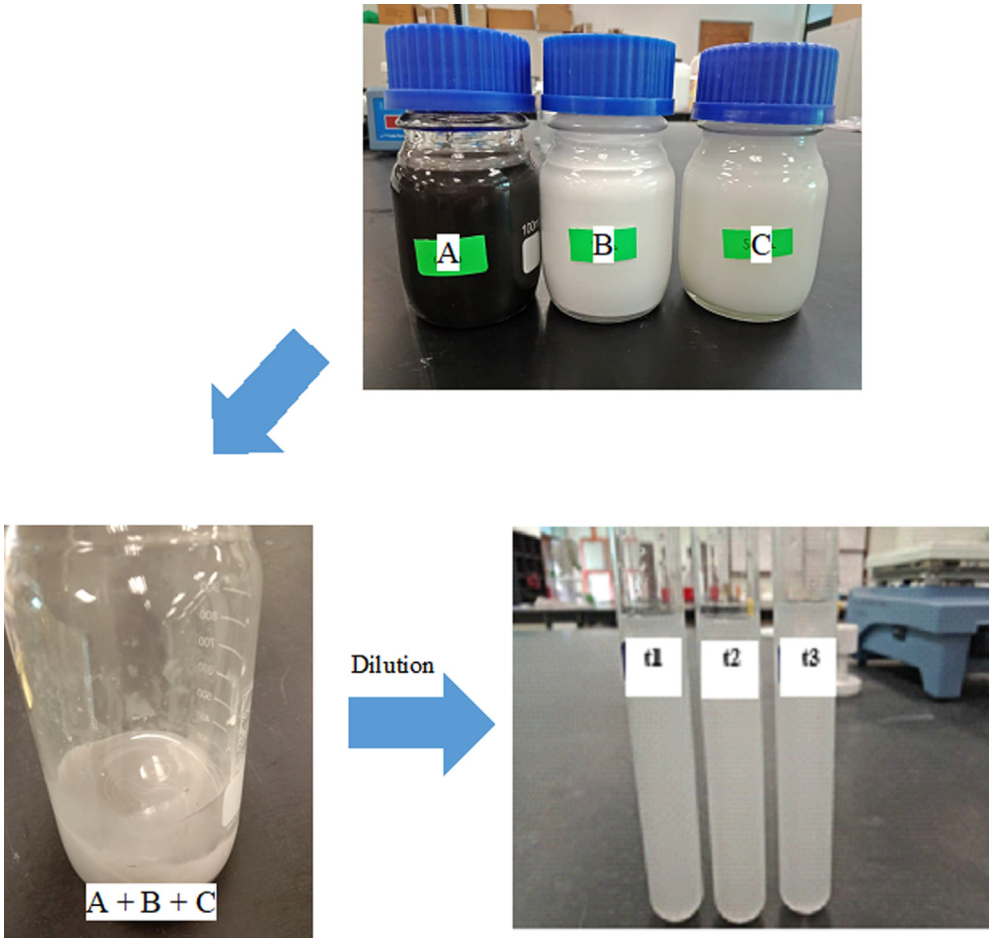

Fig. A1 Preparation of trihybrid nanofluids (**t1**, **t2**, **t3**) from CuO (A), TiO_2 (B) and SiO_2 (C).

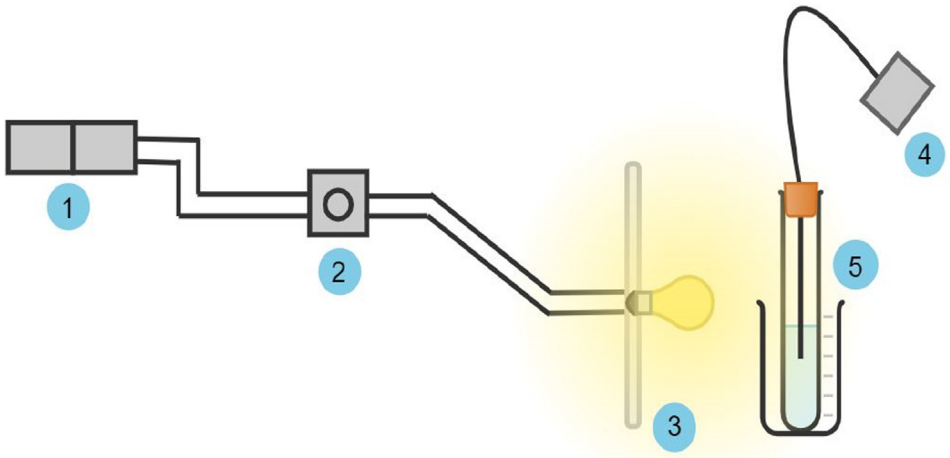

Fig. A2 The solar radiation test rig.

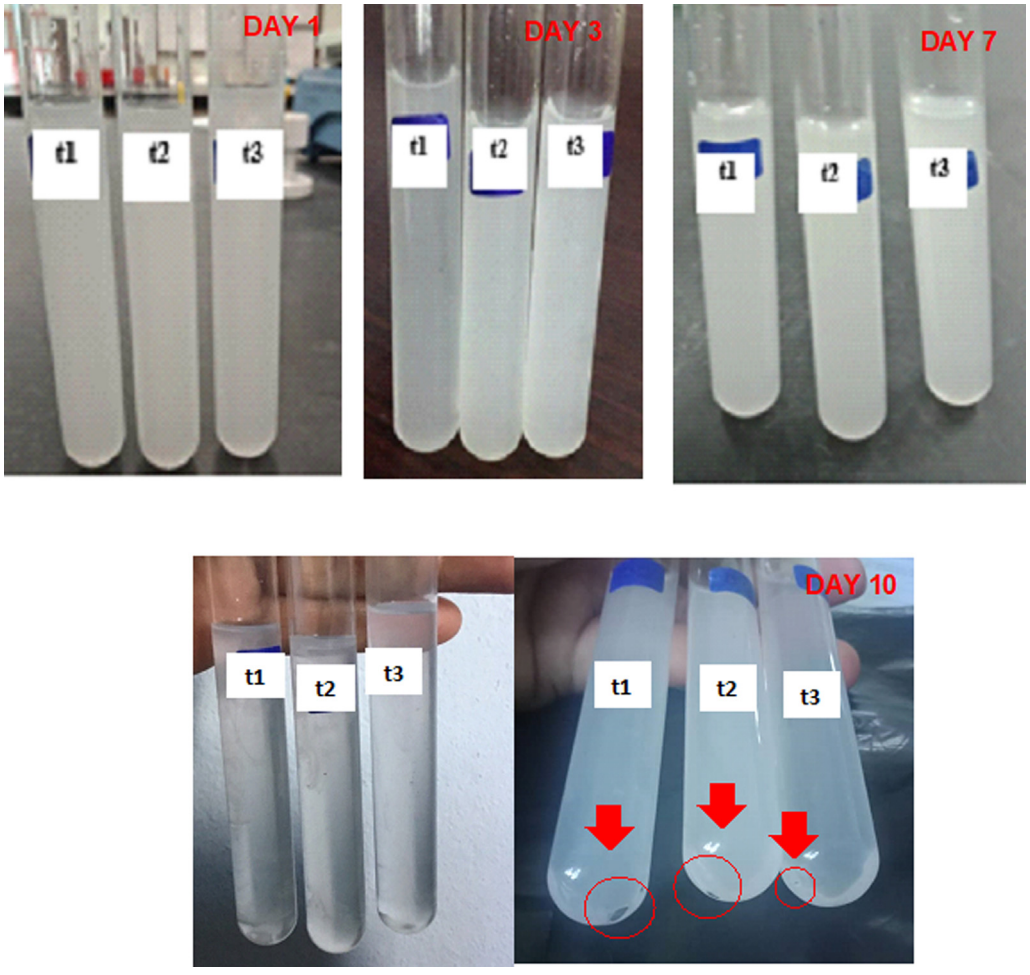

Fig. A3 Sedimentation of trihybrid nanofluids from Day 1 until Day 10, which the solutions were kept at room temperature.

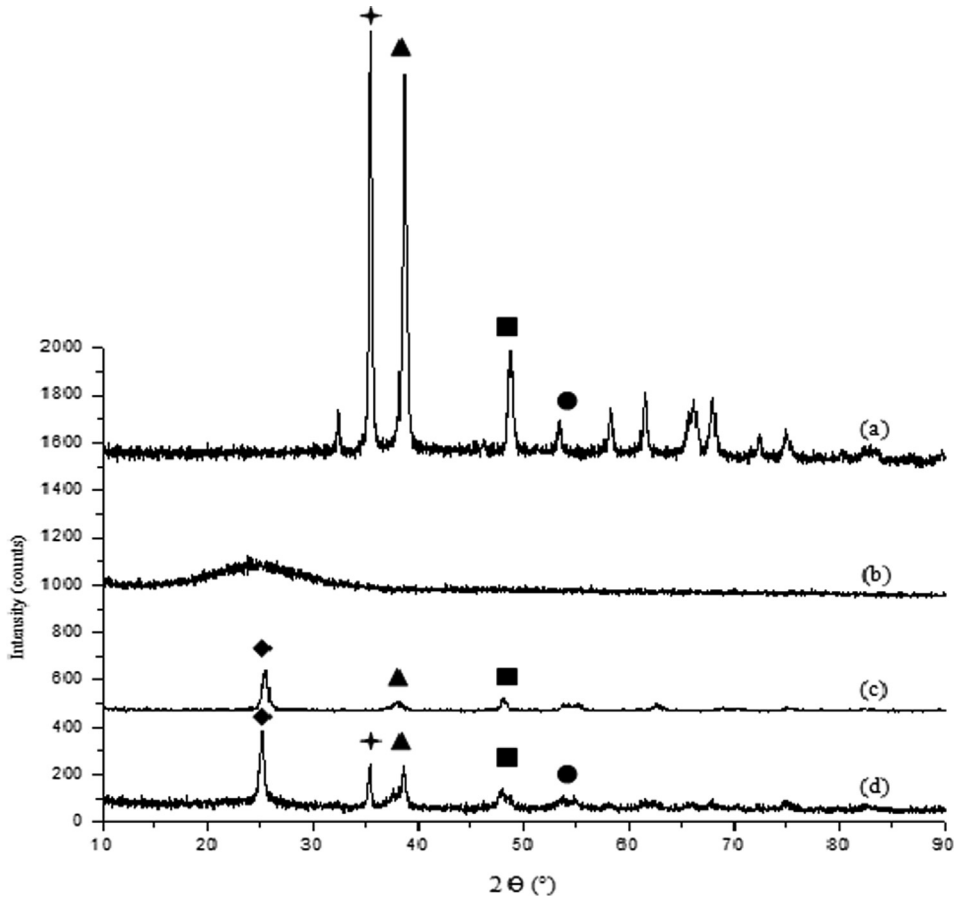

Fig. A4 XRD spectrum of (a) CuO, (b) SiO_2, (c) TiO_2 and (d) trihybrid ($CuO/SiO_2/TiO_2$).

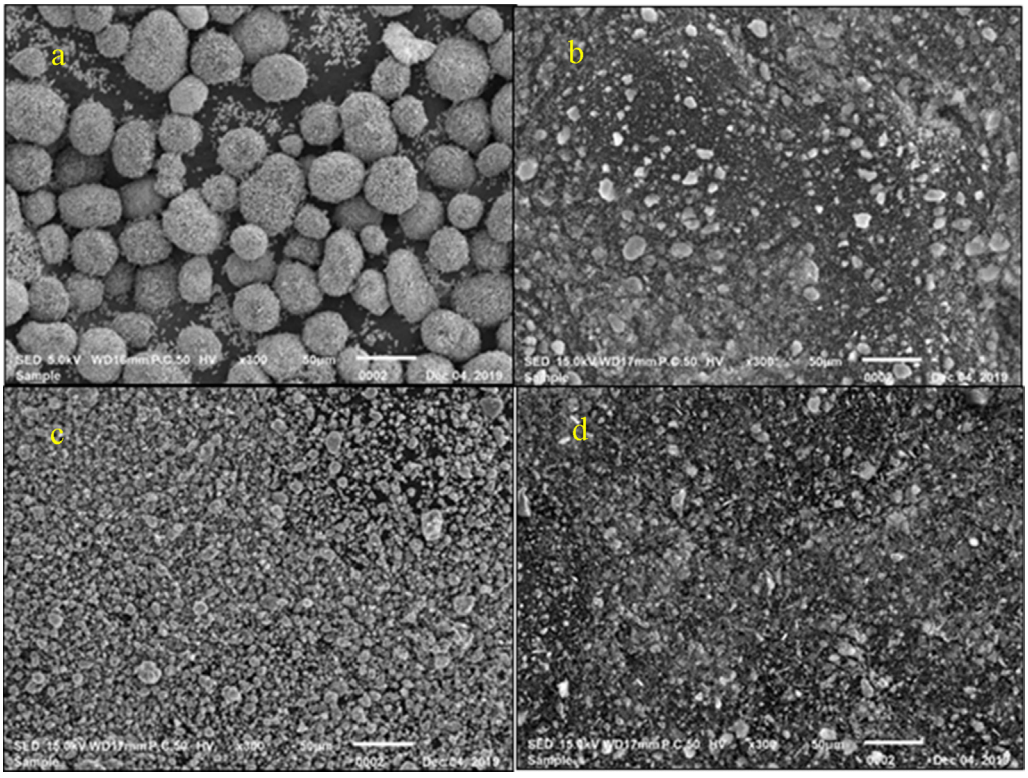

Fig. A5 Surface morphology of (a) CuO, (b) SiO_2, (c) TiO_2 and (d) trihybrid ($CuO/SiO_2/TiO_2$) at 300× magnification (50 μm).

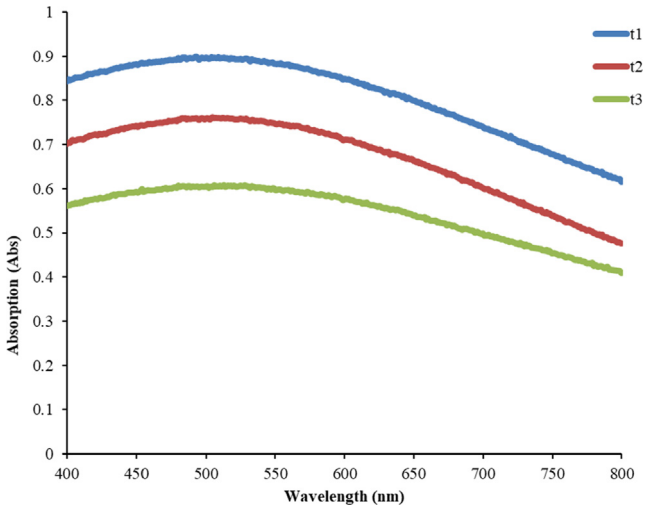

Fig. A6 UV–vis absorption of trihybrid nanofluids of **t1**, **t2** and **t3**.

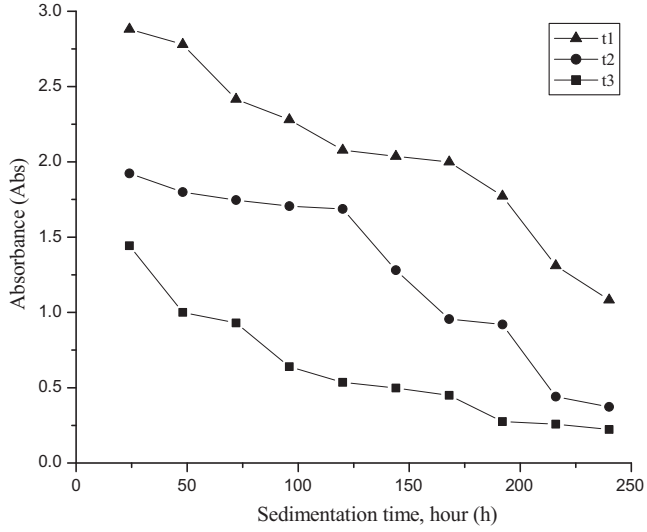

Fig. A7 The absorbance of trihybrid nanofluids up to 240 h.

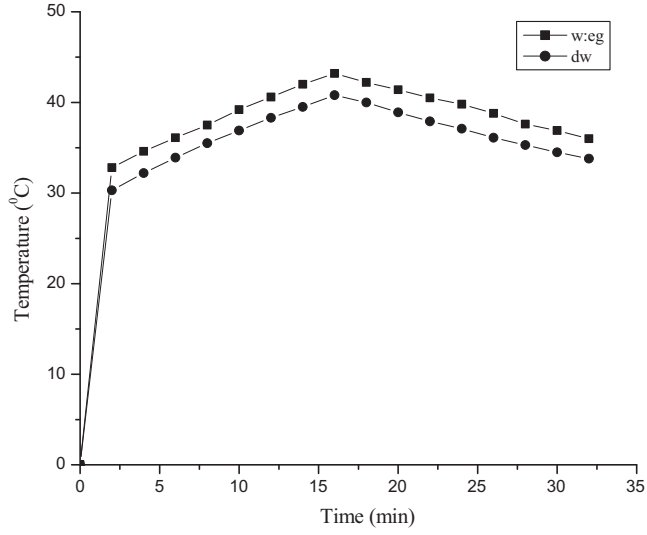

Fig. A8 Solar absorption and cooling curve of base fluids with solar radiation of 300 W/m^2.

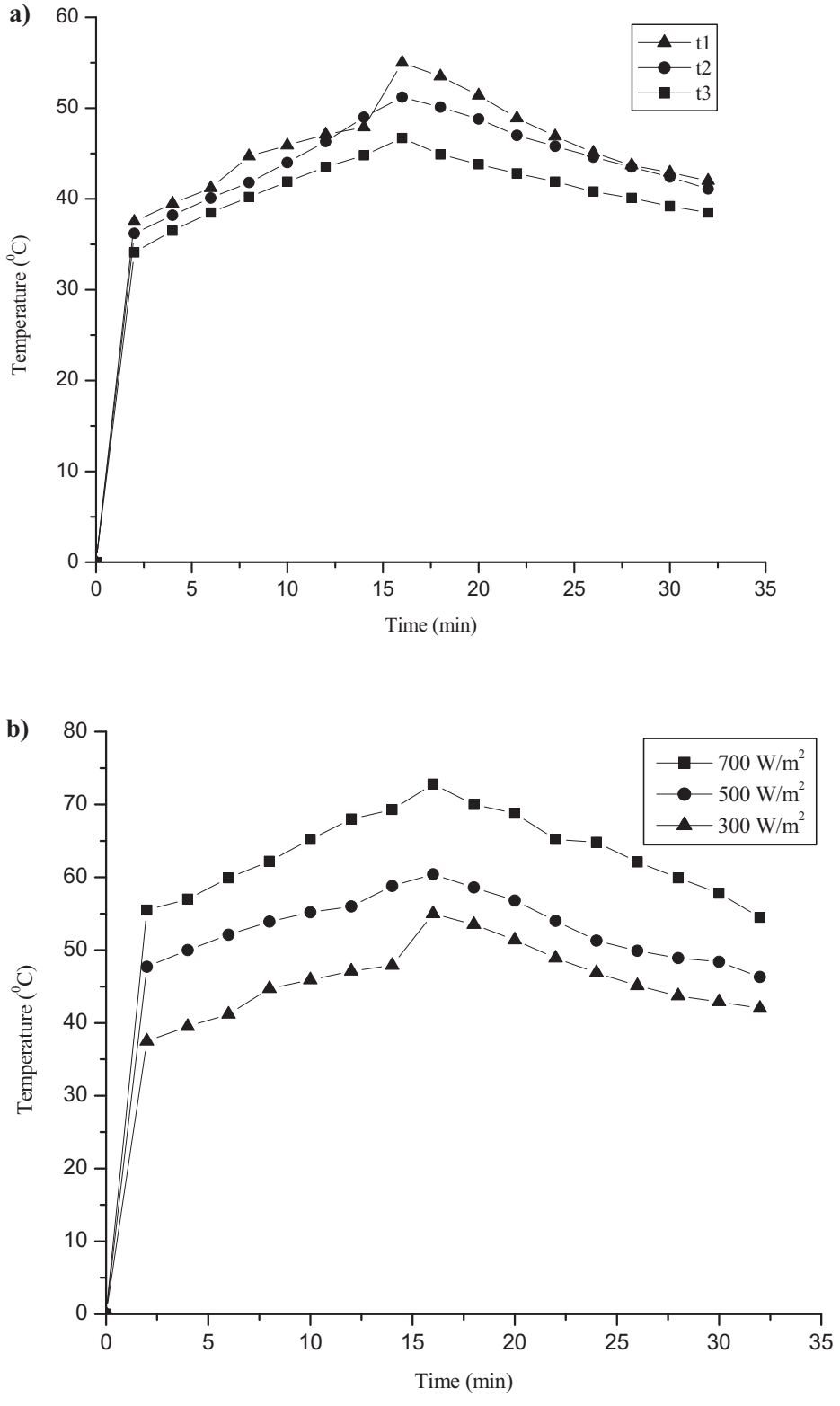

Fig. A9 Temperature output a) of the absorber based on **t1**, **t2** and **t3**, b) of **t1** with solar radiation of 300, 500 and 700 W/m^2 respectively.

Table A1 Detail description of the solar radiation test rig.

Number	Specification	Description
1	Switch Socket Outlet (Data Logger & Spotlight Dimmer)	SSO
2	Setting up with pyranometer (300 & 700 W/m^2)	Dimmer
3	Halogen 500 W	Spotlight
4	K-type	Thermocouple
5	100 mL	Test tube

Table A2 Density of base fluids and trihybrid nanofluids.

Samples	Density (g ml^{-1})
Distilled water	0.99
Water-Ethylene Glycol (60:40)	1.69
t3 trihybrid nanofluids	1.86
t2 trihybrid nanofluids	2.06
t1 trihybrid nanofluids	2.26

Table A3 The average crystallite size of nanoparticles.

Nanoparticles	CuO	SiO_2	TiO_2	Trihybrid
Peak position	35.47	24.30	25.49	25.10
FWHM	0.32	14.28	0.57	1.57
Crystallites size (nm)	26.41	0.57	14.39	5.19

Acknowledgement

Author would like to thank Faculty of Bioengineering and Technology, UMK for providing instrumentation facility.

Funding

This study was funded by UMK PRO (Grant No. R/PRO/A1300/01501A/002/2020/00759).

Appendix A. See Figs. A1–A9.

See Tables A1–A3.

References

Adam, S.A., Ju, X., Zhang, Z., Lin, J., Abd El-Samie, M.M., Xu, C., 2020. Effect of temperature on the stability and optical properties of SiO_2-water nanofluids for hybrid photovoltaic/thermal applications. Appl. Therm. Eng. 175, 115394–115405. https://doi.org/10.1016/j.applthermaleng.2020.115394.

Agarwal, R., Verma, K., Agrawal, N.K., Duchaniya, R.K., Singh, R., 2016. Synthesis, characterization, thermal conductivity and sensitivity of CuO nanofluids. Appl. Therm. Eng. 102, 1024–1036. https://doi.org/10.1016/j.applthermaleng.2016.04.051.

Akilu, S., Baheta, A.T., Sharma, K.V., 2017. Experimental measurements of thermal conductivity and viscosity of ethylene glycol-based hybrid nanofluid with TiO_2-CuO/C inclusions. J. Mol. Liq. 246, 396–405. https://doi.org/10.1016/j.molliq.2017.09.017.

Alawi, O.A., Sidik, N.A.C., Xian, H.W., Kean, T.H., Kazi, S.N., 2018. Thermal conductivity and viscosity models of metallic oxides nanofluids. Int. J. Heat Mass Transf. 116, 1314–1325. https://doi.org/10.1016/j.ijheatmasstransfer.2017.09.133.

Al-Badi, A.H., Albadi, M.H., 2012. Domestic solar water heating system in Oman: Current status and future prospects. Renew. Sust. Energ. Rev. 16, 5727–5731. https://doi.org/10.1016/j.rser.2012.06.007.

Almashhori, K., Ali, T.T., Saeed, A., Alwafi, R., Aly, M., Al-Hazmi, F.E., 2020. Antibacterial and photocatalytic activities of controllable (anatase/rutile) mixed phase TiO_2 nanophotocatalysts synthesized via a microwave-assisted sol–gel method. New J. Chem. 44 (2), 562–570. https://doi.org/10.1039/c9nj03258d.

Antić, Ž., Krsmanović, R.M., Nikolić, M.G., Marinović-Cincović, M., Mitrić, M., Polizzi, S., Dramićanin, M.D., 2012. Multisite luminescence of rare earth doped TiO_2 anatase nanoparticles. Mater. Chem. Phys. 135 (2–3), 1064–1069. https://doi.org/10.1016/j.matchemphys.2012.06.016.

Azmi, W.H., Zainon, S.N.M., Hamid, K.A., Mamat, R., 2019. A review on thermo-physical properties and heat transfer applications of single and hybrid metal oxide nanofluids. J. Mech. Eng. Sci. 13 (2), 5182–5211 https://doi.org/10.15282/jmes.13.2.2019.28.0425.

BP Statistical Review of World Energy, 2020. https://www.bp.com/content/dam/bp/business-sites/en/global/corporate/pdfs/energy-economics/statistical-review/bp-stats-review-2020-full-report.pdf (accessed 15 October 2020).

Chakraborty, S., Panigrahi, P.K., 2020. Stability of nanofluid: A review. Appl. Therm. Eng. 174 (115259), 1–26. https://doi.org/10.1016/j.applthermaleng.2020.115259.

Chakraborty, S., Sarkar, I., Ashok, A., Sengupta, I., Pal, S.K., Chakraborty, S., 2018a. Thermo-physical properties of Cu-Zn-Al LDH nanofluid and its application in spray cooling. Appl. Therm. Engi. 141, 339–351. https://doi.org/10.1016/j.applthermaleng.2018.05.114.

Chakraborty, S., Sarkar, I., Ashok, A., Sengupta, I., Pal, S.K., Chakraborty, S., 2018b. Synthesis of Cu-Al LDH nanofluid and its application in spray cooling heat transfer of a hot steel plate. Powder Technol. 335, 285–300. https://doi.org/10.1016/j.powtec.2018.05.004.

Chandrasekar, M., Suresh, S., Senthilkumar, T., 2012. Mechanisms proposed through experimental investigations on thermophysical properties and forced convective heat transfer characteristics of various nanofluids–A review. Renew. Sust. Energ. Rev. 16, 3917–3938. https://doi.org/10.1016/j.rser.2012.03.013.

Chiam, H.W., Azmi, W.H., Usri, N.A., Mamat, R., Adam, N.M., 2017. Thermal conductivity and viscosity of Al_2O_3 nanofluids for different based ratio of water and ethylene glycol mixture. Exp. Therm. Fluid Sci. 81, 420–429. https://doi.org/10.1016/j.expthermflusci.2016.09.013.

Das, S.K., Choi, S.U., Yu, W., Pradeep, T., 2007. Nanofluids: Science and Technology. John Wiley & Sons.

Deraz, N.M., Abd-Elkader, O.H., 2014. Effects of precursor on preparation and properties of nano-crystalline hopcalite particles. Asian J. Chem. 26, 2133–2137 https://doi.org/10.14233/ajchem.2014.16528.

Fikri, M.A., Asri, F.F., Faizal, W.M., Adli, H.K., Mamat, R., Azmi, W.H., Najafi, G., Yusaf, T., 2020a. TiO_2 -Si_O2 nanofluid characterization: Towards efficient with water/ethylene glycol mixture for solar application. IOP Conf. Ser. Mater. Sci. Eng. 863, 1–8. https://doi.org/10.1088/1757-899X/863/1/012055.

Fikri, M.A., Asri, F.F., Faizal, W.M., Adli, H.K., Mamat, R., Azmi, W.H., Ramadhan, A.I., Yusaf, T., 2020b. Effects of heat transfer based water for three square multilayer absorber solar collector. IOP Conf. Ser. Mater. Sci. Eng. 788 (1), 012078–012089. https://doi.org/10.1088/1757-899X/788/1/012078.

Ganji, D.D., Sabzehmeidani Y., Sedighiamiri A., 2018. Nonlinear systems in heat transfer: Chapter 3—Radiation Heat Transfer New York: Elsevier.

Ghalambaz, M., Mehryan, S.A.M., Mashoofi, N., Hajjar, A., Chamkha, A.J., Sheremet, M., Younis, O., 2020a. Free convective melting-solidification heat transfer of nano-encapsulated phase change particles suspensions inside a coaxial pipe. Adv. Powder Technol. 31 (11), 4470–4481. https://doi.org/10.1016/j.apt.2020.09.022.

Ghalambaz, M., Mehryan, S.A.M., Zahmatkesh, I., Chamkha, A., 2020b. Free convection heat transfer analysis of a suspension of nano–encapsulated phase change materials (NEPCMs) in an inclined porous cavity. Int. J. Therm. Sci. 157, 1–12. https://doi.org/10.1016/j.ijthermalsci.2020.106503.

Grätzel, M., 2009. Recent advances in sensitized mesoscopic solar cells. Acc. Chem. Res. 42, 1788–1798. https://doi.org/10.1021/ar900141y.

Guo, Y., Zhang, T., Zhang, D., Wang, Q., 2018. Experimental investigation of thermal and electrical conductivity of silicon oxide nanofluids in ethylene glycol/water mixture. Int. J. Heat Mass Transf. 117, 280–286. https://doi.org/10.1016/j.ijheatmasstransfer.2017.09.091.

Haines, A., Kovats, R.S., Campbell-Lendrum, D., Corvalán, C., 2006. Climate change and human health: impacts, vulnerability, and mitigation. Lancet 367, 2101–2109. https://doi.org/10.1016/j.puhe.2006.01.002.

Hamid, K.A., Azmi, W.H., Mamat, R., Sharma, K.V., 2019. Heat transfer performance of TiO_2–SiO_2 nanofluids in a tube with wire coil inserts. Appl. Therm. Eng. 152, 275–286. https://doi.org/10.1016/j.applthermaleng.2019.02.083.

Hamid, K.A., Azmi, W.H., Nabil, M.F., Mamat, R., 2017. Improved thermal conductivity of TiO_2–SiO_2 hybrid nanofluid in ethylene glycol and water mixture. IOP Conf. Ser. Mater. Sci. Eng. 1, 1–7. https://doi.org/10.1088/1757-899X/257/1/012067.

Hamid, K.A., Azmi, W.H., Nabil, M.F., Mamat, R., Sharma, K.V., 2018. Experimental investigation of thermal conductivity and dynamic viscosity on nanoparticle mixture ratios of TiO_2.SiO_2 nanofluids. Int. J. Heat Mass Transf. 116, 1143–1152. https://doi.org/10.1016/j.ijheatmasstransfer.2017.09.087.

Jamar, A.M.Z.A.A., Majid, Z.A.A., Azmi, W.H., Norhafana, M., Razak, A.A., 2016. A review of water heating system for solar energy applications. Int. Commun. Heat Mass Transf. 76, 178–187. https://doi.org/10.1016/j.icheatmasstransfer.2016.05.028.

Khanafer, K., Vafai, K., 2018. A review on the applications of nanofluids in solar energy field. Renew. Energy 123, 398–406. https://doi.org/10.1016/j.renene.2018.01.097.

Khedkar, R.S., Shrivastava, N., Sonawane, S.S., Wasewar, K.L., 2016. Experimental investigations and theoretical determination of thermal conductivity and viscosity of TiO_2–ethylene glycol nanofluid. Int. Commun. Heat Mass Transf. 73, 54–61. https://doi.org/10.1016/j.icheatmasstransfer.2016.02.004.

Kumar, R.S., Narukulla, R., Sharma, T., 2020. Comparative effectiveness of thermal stability and rheological properties of nanofluid of SiO_2–TiO_2 nanocomposites for oil field applications. Ind. Eng. Chem. Res. 59 (35), 15768–15783. https://doi.org/10.1021/acs.iecr.0c01944.

Li, W., Liang, R., Hu, A., Huang, Z., Zhou, Y.N., 2014. Generation of oxygen vacancies in visible light activated one-dimensional iodine TiO_2 photocatalysts. RSC Adv. 4 (70), 36959–36966. https://doi.org/10.1039/C4RA04768K.

Minea, A.A., 2017. Hybrid nanofluids based on Al_2O_3, TiO_2 and SiO_2: numerical evaluation of different approaches. Int. Commun. Heat Mass Transf. 104, 852–860. https://doi.org/10.1016/j.ijheatmasstransfer.2016.09.012.

Mohammadi, M., Dadvar, M., Dabir, B., 2017. TiO_2/SiO_2 nanofluids as novel inhibitors for the stability of asphaltene particles in crude oil: Mechanistic understanding, screening, modeling, and optimization. J. Mol. Liq. 238, 326–340. https://doi.org/10.1016/j.molliq.2017.05.014.

Moldoveanu, G.M., Huminic, G., Minea, A.A., Huminic, A., 2018. Experimental study on thermal conductivity of stabilized Al_2O_3 and SiO_2 nanofluids and their hybrid. Int. J. Heat Mass Transf. 127, 450–457. https://doi.org/10.1016/j.ijheatmasstransfer.2018.07.024.

Nabil, M.F., Azmi, W.H., Hamid, K.A., Mamat, R., 2018. Experimental investigation of heat transfer and friction factor of TiO_2-SiO_2 nanofluids in water: ethylene glycol mixture. Int. Commun. Heat Mass Transf. 124, 1361–1369. https://doi.org/10.1016/j.ijheatmasstransfer.2018.04.143.

Nayak, P.P., Nandi, S., Datta, A.K., 2019. Comparative assessment of chemical treatments on extraction potential of commercial grade silica from rice husk. Eng. Rep. 1, 1–13. https://doi.org/10.1002/eng2.12035.

Nemale, K., Waghuley, S., 2016. A novel approach for enhancement of thermal conductivity of CuO/H_2O based nanofluids. Appl. Therm. Eng. 95, 271–274. https://doi.org/10.1016/j.applthermaleng.2015.11.053.

Okonkwo, E.C., Wole-Osho, I., Kavaz, D., Abid, M., 2019. Comparison of experimental and theoretical methods of obtaining the thermal properties of alumina/iron mono and hybrid nanofluids. J. Mol. Liq. 292, 111377–111394. https://doi.org/10.1016/j.molliq.2019.111377.

Peyghambarzadeh, S.M., Hashemabadi, S.H., Hoseini, S.M., Jamnani, M.S., 2011. Experimental study of heat transfer enhancement using water/ethylene glycol based nanofluids as a new coolant for car radiators. Int. Commun. Heat Mass Transf. 38, 1283–1290. https://doi.org/10.1016/j.icheatmasstransfer.2011.07.001.

Ramadhan, A.I., Azmi, W.H., Mamat, R., 2020. Heat transfer characteristics of car radiator using tri-hybrid nanocoolant. IOP Conf. Ser. Mater. Sci. Eng. 863 (1), 012054–012064. https://doi.org/10.1088/1757-899X/863/1/012054.

Ramadhan, A.I., Azmi, W.H., Mamat, R., Hamid, K.A., Norsakinah, S., 2019. Investigation on stability of tri-hybrid nanofluids in water-ethylene glycol mixture. IOP Conf. Ser. Mater. Sci. Eng. 469 (1), 1–9. https://doi.org/10.1088/1757-899X/469/1/012068.

Ranjbar-Karimi, R., Bazmandegan-Shamili, A., Aslani, A., Kaviani, K., 2010. Sonochemical synthesis, characterization and thermal and optical analysis of CuO nanoparticles. Physica B: Condens. Matter 405, 3096–3100. https://doi.org/10.1016/j.physb.2010.04.021.

Safiei, W., Rahman, M.M., Musfirah, A.H., Maleque, M.A., Singh, R., 2020. Experimental study on dynamic viscosity of aqueous-based nanofluids with an addition of ethylene glycol. IOP Conf. Ser., Mater. Sci. Eng. 788 (1), 012094-012103. IOP Publishing. https://doi.org/10.1088/1757-899X/788/1/012094.

Sahid, N.S.M., Rahman, M.M., Kadirgama, K., Maleque, M.A., 2017. Experimental investigation on properties of hybrid nanofluids (TiO_2 and ZnO) in water–ethylene glycol mixture. J. Mech. Eng. Sci. 11, 3087–3094 https://doi.org/10.15282/jmes.11.4.2017.11.0277.

Saidina, D.S., Abdullah, M.Z., Hussin, M., 2020. Metal oxide nanofluids in electronic cooling: a review. J. Mater. Sci. Mater. Electron. 31, 4381–4398. https://doi.org/10.1007/s10854-020-03020-7.

Sarafraz, M.M., Arya, A., Nikkhah, V., Hormozi, F., 2016. Thermal performance and viscosity of biologically produced silver/coconut oil nanofluids. Chem. Biochem. Eng. Q. 30 (4), 489–500 https://doi.org/10.15255/CABEQ.2015.2203.

Sarafraz, M.M., Arya, H., Arjomandi, M., 2018. Thermal and hydraulic analysis of a rectangular microchannel with gallium-copper oxide nano-suspension. J. Mol. Liq. 263, 382–389. https://doi.org/10.1016/j.molliq.2018.05.026.

Sarafraz, M.M., Safaei, M.R., Tian, Z., Goodarzi, M., Bandarra Filho, E.P., Arjomandi, M., 2019. Thermal assessment of nano-particulate graphene-water/ethylene glycol (W/EG 60:40) nano-suspension in a compact heat exchanger. Energies 12, 1–17. https://doi.org/10.3390/en12101929.

Sharif, M.Z., Azmi, W.H., Redhwan, A.A.M., Mamat, R., Najafi, G., 2019. Energy saving in automotive air conditioning system perfor-

mance using SiO_2/PAG nanolubricants. J. Therm. Anal. Calorim. 135, 1285–1297. https://doi.org/10.1007/s10973-018-7728-3.

Shukla, R., Sumathy, K., Erickson, P., Gong, J., 2013. Recent advances in the solar water heating systems: A review. Renew. Sust. Energ. Rev. 19, 173–190. https://doi.org/10.1016/j.rser.2012.10.048.

Siddiqui, H., Parra, M.R., Qureshi, M.S., Malik, M.M., Haque, F.Z., 2018. Studies of structural, optical, and electrical properties associated with defects in sodium-doped copper oxide (CuO/Na) nanostructures. J. Mater. Sci. 53 (12), 8826–8843. https://doi.org/10.1007/s10853-018-2179-6.

Sonawane, S.S., Khedkar, R.S., Wasewar, K.L., 2015. Effect of sonication time on enhancement of effective thermal conductivity of nano TiO_2–water, ethylene glycol, and paraffin oil nanofluids and models comparisons. J. Exp. Nanosci. 10 (4), 310–322. https://doi.org/10.1080/17458080.2013.832421.

Subramaniyan, A., Thiruppathi, S., Sathath, M.I.M., 2018. Investigation on band gap of CuO–ZnO nanocomposite thin films and stability of CuO–ZnO nanofluids. J. Nanoelectron. Optoelectron. 13, 1366–1373. https://doi.org/10.1166/jno.2018.2360.

Sundar, L.S., Ramana, E.V., Singh, M.K., Sousa, A.C., 2014. Thermal conductivity and viscosity of stabilized ethylene glycol and water mixture Al_2O_3 nanofluids for heat transfer applications: An experimental study. Int. Comm. Heat Mass Transf. 56, 86–95. https://doi.org/10.1016/j.icheatmasstransfer.2014.06.009.

Tahat, M.S., Benim, A.C., 2017. Experimental analysis on thermophysical properties of Al_2O_3/CuO hybrid nano fluid with its effects on flat plate solar collector. Defect Diffus. Forum 374, 148–156. https://doi.org/10.4028/www.scientific.net/DDF.374.148.

Toghraie, D., Chaharsoghi, V.A., Afrand, M., 2016. Measurement of thermal conductivity of ZnO–TiO_2/EG hybrid nanofluid. J. Therm. Anal. Calorim 125 (1), 527–535. https://doi.org/10.1007/s10973-016-5436-4.

Urmi, W., Rahman, M.M., Hamzah, W.A.W., 2020. An experimental investigation on the thermophysical properties of 40% ethylene glycol based TiO_2-Al_2O_3 hybrid nanofluids. Int. Commun. Heat Mass Transf. 116, 104663–104676. https://doi.org/10.1016/j.icheatmasstransfer.2020.104663.

Wanatasanapan, V.V., Abdullah, M.Z., Gunnasegaran, P., 2020. Effect of TiO_2-Al_2O_3 nanoparticle mixing ratio on the thermal conductivity, rheological properties, and dynamic viscosity of water-based hybrid nanofluid. J. Mater. Res. Technol. 9 (6), 13781–13792. https://doi.org/10.1016/j.jmrt.2020.09.127.

Yuvakkumar, R., Elango, V., Rajendran, V., 2014. High-purity nano silica powder from rice husk using a simple chemical method. J. Exp. Nanosci. 9, 272–281. https://doi.org/10.1080/17458080.2012.656709.

Zak, A.K., Majid, W.A., Abrishami, M.E., Yousefi, R., Parvizi, R., 2012. Synthesis, magnetic properties and X-ray analysis of $Zn_{0.97}$-$X_{0.03}O$ nanoparticles (X = Mn, Ni, and Co) using Scherrer and size–strain plot methods. Solid State Sci. 14 (4), 488–494. https://doi.org/10.1016/j.solidstatesciences.2012.01.019.

Żyła, G., Fal, J., 2017. Viscosity, thermal and electrical conductivity of silicon dioxide–ethylene glycol transparent nanofluids: An experimental studies. Thermochimica acta 650, 106–113. https://doi.org/10.1016/j.tca.2017.02.001.